

AD-A185 386

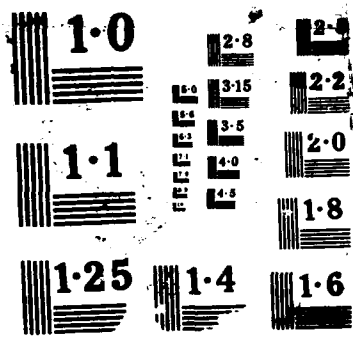
THE POLAR IONOSPHERE AND INTERPLANETARY FIELD(U) ALASKA 1/1
UNIV FAIRBANKS GEOPHYSICAL INST B J WATKINS ET AL
AUG 87 AFOSR-TR-87-1342 \$AFOSR-85-0258

UNCLASSIFIED

F/G 4/1

NL

FND
11/87
D10



AD-A185 386

DOCUMENTATION PAGE DTIC FILE COPY

Form Approved
OMB No. 0704-0188

1a. REPORT SECURITY CLASSIFICATION Unclassified			1b. RESTRICTIVE MARKINGS	
2a. SECURITY CLASSIFICATION SELECTED			3. DISTRIBUTION/AVAILABILITY OF REPORT Approved for public release; Distribution Unlimited	
2b. DECLASSIFICATION/DOWNGRADING SCHEDULE SCHEDULE 1 1987			5. MONITORING ORGANIZATION REPORT NUMBER(S) AFOSR-TR- 87-1342	
4. PERFORMING ORGANIZATION REPORT NUMBER(S) CA2 D			7a. NAME OF MONITORING ORGANIZATION AFOSR/NC	
6a. NAME OF PERFORMING ORGANIZATION Geophysical Institute		6b. OFFICE SYMBOL (If applicable)		7b. ADDRESS (City, State, and ZIP Code) Bldg. 410 Bolling AFB, DC 20332-6448
6c. ADDRESS (City, State, and ZIP Code) University of Alaska Fairbanks, AK 99775-0800		9. PROCUREMENT INSTRUMENT IDENTIFICATION NUMBER AFOSR-85-0258		
8a. NAME OF FUNDING/SPONSORING ORGANIZATION AFOSR		8b. OFFICE SYMBOL (If applicable) NC		10. SOURCE OF FUNDING NUMBERS
8c. ADDRESS (City, State, and ZIP Code) Bldg. 410 Bolling AFB DC 20332-6448		PROGRAM ELEMENT NO. 61102F PROJECT NO. 2310 TASK NO. A2 WORK UNIT ACCESSION NO.		
11. TITLE (Include Security Classification) The Polar Ionosphere and Interplanetary Field				
12. PERSONAL AUTHOR(S) B.J. Watkins and S-I. Akasofu				
13a. TYPE OF REPORT Final Technical		13b. TIME COVERED FROM 1 Jul 85 to 30 Jun 87		14. DATE OF REPORT (Year, Month, Day) August 1987
15. PAGE COUNT 40				
16. SUPPLEMENTARY NOTATION				
17. COSATI CODES			18. SUBJECT TERMS (Continue on reverse if necessary and identify by block number)	
FIELD	GROUP	SUB-GROUP	Ionosphere, Magnetosphere, Interplanetary Magnetic Field, Model, geomagnetic storm, polar F-region	
19. ABSTRACT (Continue on reverse if necessary and identify by block number) The model ionosphere was developed that is coupled to a magnetospheric model for investigating time dependent behavior of the Polar F-region ionosphere in response to varying interplanetary magnetic field (IMF) configurations. The numerical ionospheric model covers a latitude range from 50 to 90 degrees and an altitude range of 150 to 600 KM. The purpose of the magnetospheric model is to define the location and geometry of the polar cap, which is defined as the region of open field lines. The polar cap configuration has been coupled				
20. DISTRIBUTION/AVAILABILITY OF ABSTRACT <input checked="" type="checkbox"/> UNCLASSIFIED/UNLIMITED <input checked="" type="checkbox"/> SAME AS RPT. <input type="checkbox"/> DTIC USERS			21. ABSTRACT SECURITY CLASSIFICATION Unclassified	
22a. NAME OF RESPONSIBLE INDIVIDUAL JAMES P. KOERMER, Lt Col, USAF			22b. TELEPHONE (Include Area Code) (202) 767-4960	22c. OFFICE SYMBOL NC

DD Form 1473, JUN 86

Previous editions are obsolete.

SECURITY CLASSIFICATION OF THIS PAGE

87 9 24 309

to a model electric field pattern that in turn may vary in size and strength in response to the IMF. The ionosphere model assumes only oxygen ions; the ion density is solved vertically along many magnetic field lines as they move horizontally under the influence of the large-scale convective electric fields. The lower boundary is defined by the local chemistry and the upper boundary condition has been set by applying an outward flux of ions appropriate for open field line conditions. The model has been used to illustrate ionospheric behavior during geomagnetic storms conditions. Future model applications may include ionospheric prediction using IMF inputs improved understanding of polar ionization structures.

SEP 10 1987

AFOSR-TR- 87 - 1342

FINAL REPORT

Grant AFOSR-85-0285

THE POLAR IONOSPHERE AND INTERPLANETARY FIELD

B.J. Watkins and S.-I. Akasofu
Geophysical Institute
University of Alaska



Accession For	
NTIS CR&I	<input checked="checked" type="checkbox"/>
DTIC TAB	<input type="checkbox"/>
Unannounced	<input type="checkbox"/>
Justification	
By	
Date	
Availability Codes	
DIST	1. 2. 3. 4. 5. 6. 7. 8. 9. 10. 11. 12.
A-1	

August 1987

Approved for public release,
distribution unlimited

CONTENTS

1. RESEARCH RESULTS

1.1 Objectives

1.2 Model Development

1.2.1 Magnetosphere Model

1.2.2 O^+ Ion Equations

1.2.3 Auroral Ionization

1.3 Current Status of Model

1.4 Model Application

1.4.1 Ionospheric Response to a Geomagnetic Storm

2. PLANNED MODEL EXTENSIONS AND APPLICATIONS

3. PERSONNEL

4. EXTERNAL INTERACTIONS

4.1 Conference Presentations

4.2 Publications

4.3 Participation in CEDAR program

5. CONCLUSIONS

REFERENCES

SUMMARY

We have developed a model ionosphere that is coupled to a magnetosphere model for investigating time dependent behavior of the polar F-region ionosphere in response to varying interplanetary magnetic field (IMF) configurations. The numerical ionospheric model covers a latitude range from 50 to 90 degrees, and an altitude range 150 to 600km. The purpose of the magnetosphere model is to define the location and geometry of the polar cap, which is defined as the region of open field lines. The polar cap configuration has been coupled to a model electric field pattern that in turn may vary in size and strength in response to the IMF. The ionosphere model assumes only oxygen ions, the ion density is solved vertically along many magnetic field lines as they move horizontally under the influence of the large-scale convective electric fields. The lower boundary is defined by the local chemistry, the upper boundary condition has been set by applying an outward flux of ions (which is appropriate for open field line conditions). The model has been applied to illustrate ionospheric behavior during geomagnetic storm conditions. Future use of this model may have applications in predicting ionospheric conditions using IMF inputs, and to enhance basic understanding of polar ionization structures.

1. RESEARCH RESULTS

1.1 OBJECTIVES

This grant period began with a simple subroutine that computed the ion density along field lines, and a first attempt at combining this with a model electric field structure. The overall objective was to build on this basis to develop a new three-dimensional time dependent model of the polar ionosphere. In doing this, it was planned to incorporate as much of the basic physics and chemistry as possible, but to omit secondary effects. Since computer resources, no matter how abundant, never seem adequate, it has been our philosophy to only model the basic processes responsible for the F-region structure and to keep an appropriate balance between modeling from first principles and parameterization; thus computer time has been minimized. This has been achieved by carefully constructing our computer codes, and to keep the modeled processes about equal in importance. For example, it is wasteful to spend considerable effort and precision in calculating one quantity such as auroral ionization, if other equally important production functions such as photoionization can not be determined with a high degree of certainty. Thus, a number of compromises have been made to keep the computational times reasonable; these can be adjusted in future as better experimental inputs are incorporated.

There are still some minor objectives that could not be accomplished in the grant period and these are mentioned in section 2. The major goal of coupling an ionospheric model to magnetospheric inputs has been accomplished. We are now able to study the time dependent behavior of the polar ionosphere in response to varying interplanetary field (IMF) values. It needs to be clearly stated however, that this is a first attempt and several improvements are still possible. It was not an objective to predict or simulate a real ionosphere; there have been no comparisons with real data. However, further development and application of this work should be useful for future comparisons with data, using the model to investigate basic physical processes, and to predict ionospheric conditions with magnetospheric inputs. The main objectives accomplished were:

- Set up a magnetospheric model to compute the polar cap size and position. The model of Akasofu and Roederer(1984) has been adopted and modified for our purposes.
- Define a model for the large scale convective electric fields. This model is scaled to match the polar cap configuration that results from the magnetospheric model.
- Write new code to compute ion densities vertically along magnetic field lines.
- Devise an efficient method to track individual field lines as they move horizontally under the influence of the convective electric fields.
- Write code to compute auroral ionization from particle flux data.
- Write efficient code to compute photoionization rates.
- Combine all computer codes into a package that responds to IMF inputs and generate a time sequence of ionospheric structures.

1.2 MODEL DEVELOPMENT

The approach to the model development has been to focus on the interactions of the ionosphere with the magnetosphere, particularly the dynamics of the auroral oval and polar cap. The function of the magnetosphere model is to define the region of open field lines and the auroral oval in response to the interplanetary field (IMF). A model of the large scale convective electric fields is scaled to the location and size of the polar cap. In this way it has been possible to develop a time dependent simulation of the polar ionosphere and to follow its response to time varying IMF values.

The determination of the ionospheric convection pattern follows from several steps. First, the IMF is used as an input to the magnetospheric model which gives the location and size of the polar cap. For the purposes of this model, the polar cap is defined as the region of open field lines; by contrast, some authors refer to the polar cap as the region inside the discrete auroral oval that contains no visible aurora. The polar cap from the model is approximately circular for conditions of southward IMF, and a best fit circle is then used to define the polar cap for the ionospheric modeling. Conditions of northward IMF are uncertain because observations have not yet clearly defined the electric field structure during these periods. The edge of the polar cap is assumed to be the poleward boundary of the auroral oval precipitation. The equatorward auroral boundary has been determined using an empirical expression that has been derived from statistical observations of aurora; examples are shown in section 1.4 .

The total cross polar cap potential is determined from the ϵ parameter which is given by,

$$\epsilon = v B^2 \sin^4(\theta/2) l_0^2$$

where v is the solar wind speed, B is the IMF magnitude, θ is the polar angle of the IMF vector, and l_0 is a constant of about 7 earth radii. Reif et al (1981) have determined an empirical relationship between ϵ and the cross polar cap potential Φ to be,

$$\Phi = 0.93 \epsilon - 319$$

Thus, the IMF (the vector components) and ϵ are being used as the model inputs. These in turn define the size and position of the auroral oval and polar cap, and the magnitude and morphology of the large scale convective electric fields.

The plasma motions are given by the vector $\mathbf{E} \times \mathbf{B}$ motions, however the small vertical $\mathbf{E} \times \mathbf{B}$ component is neglected. It is important to note that the problem is solved in the non-rotating magnetosphere reference frame using magnetic local time and magnetic latitude coordinates. The computations of ion densities are made in this frame, but transformations to the geographic frame are made to compute photoionization rates because the solar zenith angle is dependent on the geographic location.

For the ion calculations it is assumed that O^+ is the only ion, which is a good approximation. The continuity and momentum equations are solved vertically along the inclined magnetic field lines. An upper boundary condition at 600km is set with an outward ion flux over the polar cap, the lower boundary at 150km is set by the appropriate local chemistry. The height of the lower boundary was chosen at 150km because this is approximately the lowest height that plasma moves under $\mathbf{E} \times \mathbf{B}$ motions. Below this height the ionization is more easily determined because the recombination time is short and the densities are determined by the local production. In the F-region where recombination times are well in excess of an hour, the ionization densities at a particular location depend on the past history of production and loss processes on the field line. This is the reason why a large-scale model must be used to determine and predict the ionization at a particular location. For example, plasma densities in the nighttime auroral zone may be produced on the dayside of the earth and then transported across the polar cap to the nightside before significant recombination has taken place.

The approach used to simulate a time varying ionosphere is to first generate a reasonable starting value ionosphere. This is done by back-tracking each location in time to determine where the plasma originated from 4 hours earlier. Then, from this earlier location, a field line is time stepped to its position of interest. The ion equation is solved about every minute along the field line. This procedure is repeated for many locations (ie different field lines) to build up a three-dimensional structure. This three-dimensional structure is then stored and allowed to evolve in time by further tracking field lines. For the example shown in section 1.4.1 the ionospheric structure is plotted every hour, however the time steps for individually solving the ion equations are very short, typically a minute or less.

In the next three sections more aspects of the magnetosphere model, ion equation solutions, and auroral inputs are discussed.

1.2.2 MAGNETOSPHERE MODEL

Examples of this magnetospheric model have been shown by Akasofu and Roederer(1984). The model has been adapted for compatibility and rapid computational time when used in conjunction with the ionospheric model. The major remaining question with the model is the behavior under northward IMF conditions. There remains some uncertainty from spacecraft observations (mainly due to the paucity of data) about the northward IMF structure for both open field line and electric field structures.

There is an important point regarding the application of the upper boundary condition flux that is relevant to the magnetosphere model. Over the polar cap, field lines are open and a continual outward flux has been used; this should be an excellent assumption. However, on closed field lines in the plasmasphere this is not the case. The field-aligned flow in or out of the ionosphere depends on the ionization densities in the plasmasphere, which in turn depends on the past history of field line filling/emptying for perhaps a day or more. Other researchers with large scale ionospheric models seem to have avoided this problem. This is very important on the nightside post-midnight auroral zone where ionospheric densities are low and magnetic field lines are closed. The modeling work so far has assumed a zero flux in the closed field line region. This is an area that must be addressed in future work because ionospheric densities may easily be affected by factors of 2 or 3 depending on the particular time and geophysical conditions.

1.2.2 SOLUTION OF THE O^+ ION EQUATION

The following symbols are used in this section.

n = ion number density, only oxygen ions are assumed (m^{-3})

N_e = electron number density

T_i = ion temperature

T_e = electron temperature

$T_p = T_i + T_e$ plasma temperature (note, some authors define $T_p = (T_i + T_e)/2$)

$H_p = (k T_p)/(M_i g)$ scale height (m)

k = Boltzman constant (mks units)

M_i = ion mass (in Kg)

g = gravitational acceleration (m/s)

$D = D_a \sin^2 I$ vertical diffusion coefficient

$D_a = (k T_p / M_i v_i)$ ambipolar diffusion coefficient

$v_i = \sum_n v_{in}$ = ion-neutral collision frequency summed over all species

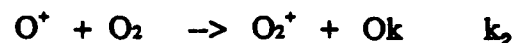
I = magnetic dip angle, positive in the northern hemisphere

w_D = vertical drift induced by neutral winds

p = production rate

β = electron recombination rate coefficient

The continuity and momentum equations for O^+ ions has been solved for the altitude range 150 to 600 km. The lower boundary is determined by the local chemistry with diffusion being negligible. The upper boundary condition is set by an ion flux, which is always upward in the polar cap; at lower latitudes it may be upward, downward, or zero. The relevant chemistry operating over the F-region ionosphere to destroy electrons and O^+ ions is:



The loss coefficient therefore becomes:

$$\beta = \left[\frac{k_1 [N_2] + K_2 [O_2]}{1 + \frac{k_2 [O_2]}{a_1 N_e} + \frac{k_1 [N_2]}{a_2 N_e}} \right]$$

The loss rate of ions is therefore βn .

The continuity and momentum equations are respectively,

$$\partial n / \partial t + \partial(nw) / \partial z = p - \beta n$$

$$w = w_D - D \left((1/n) \partial n / \partial z + (1/T_p) \partial T_p / \partial z + (1/H_p) \right)$$

The momentum and continuity equations may be combined to yield a diffusion equation,

$$\partial n / \partial t + \partial \left[n w_D - D \partial n / \partial z - (D n / T_p) \partial T_p / \partial z - (D n) / H_p \right] / \partial z = p - \beta n$$

Taking derivatives, the following are obtained,

$$\begin{aligned} \text{where} \quad \partial^2 n / \partial z^2 &= f_4 \partial n / \partial t + f_1 \partial n / \partial z + f_2 n + f_3 \\ f_1 &= -(1/D) \partial D / \partial t - (1/T_p) \partial T_p / \partial z - 1/H_p + w_D / D \\ f_2 &= -((1/T_p) \partial T_p / \partial t) ((1/D) \partial D / \partial z) - (1/T_p) \partial^2 T_p / \partial z^2 \\ &\quad + ((1/T_p) \partial T_p / \partial z)^2 - (1/H_p) ((1/D) \partial D / \partial z) \\ &\quad + ((1/H_p) ((1/H_p) (\partial H_p / \partial z)) + ((1/D) (\partial w_D / \partial z) \\ &\quad + \beta / D \\ f_3 &= -p / D \\ f_4 &= 1 / D \end{aligned}$$

With the equations in this format, the Crank-Nicholson method with a predictor-corrector type modification has been used for their solution. The predictor is given by,

$$\Delta z^2 n_{i,j+1/2} = f_{4,i,j} \Delta t^2 (n_{i,j+1/2} - n_{i,j}) + f_{1,i,j} \Delta n_{i,j} + f_{2,i,j} n_{i,j} + f_{3,i,j}$$

$$\text{where } \Delta x^2 n_i = (n_{i+1} - 2n_i + n_{i-1}) / (\Delta x)^2$$

$$\text{and } \Delta x n_i = (n_{i+1} - n_{i-1}) / 2\Delta x$$

Rearranging, then substituting the difference operators that operate on the $n_{j+1/2}$ results in,

$$\begin{aligned} (1/\Delta z)^2 n_{i-1,j+1/2} - 2((1/\Delta z)^2 + (f_{4,i,j} / \Delta t)) n_{i,j+1/2} + (1/\Delta z)^2 n_{i+1,j+1/2} \\ = (f_{2,i,j} - (2f_{4,i,j} / \Delta t)) n_{i,j} + f_{1,i,j} \Delta z n_{i,j} + f_{3,i,j} \end{aligned} \quad (0a)$$

The corrector is given by ,

$$\begin{aligned} (1/2) \Delta z^2 (n_{i,j+1} + n_{i,j}) &= f_{4,i,j+1/2} (1/\Delta t) (n_{i,j+1} - n_{i,j}) \\ &\quad + (1/2) f_{1,i,j+1/2} \Delta t (n_{i,j+1} + n_{i,j}) \\ &\quad + f_{2,i,j+1/2} n_{i,j+1/2} + f_{3,i,j} \end{aligned}$$

This results in,

$$\begin{aligned}
 & \left(\frac{1}{\Delta z} \right)^2 + \left(\frac{1}{2} \Delta z \right) f_{i,j+1/2} \Big) - 2 \left(\frac{1}{\Delta z} \right)^2 + f_{i,j+1/2} / \Delta t \Big) n_{i,j+1/2} \\
 & + \left(\frac{1}{\Delta z} \right)^2 - \left(\frac{1}{2} \Delta z \right) f_{i,j+1/2} \Big) n_{i+1,j+1} \\
 & = 2 \left(f_{i,j+1/2} n_{i,j+1/2} + f_{i,j+1/2} - \left(f_{i,j+1/2} n_{i,j} \right) / \Delta t \right) \\
 & + f_{i,j+1/2} \Delta z n_{i,j} - \Delta z^2 n_{i,j}
 \end{aligned} \tag{0b}$$

The right hand side of the predictor is completely known, therefore the left-hand side defines a tridiagonal system in the $n_{i,j+1/2}$ variable. Similarly, the corrector defines a tridiagonal system in the n_{j+1} variable once the $n_{j+1/2}$ variables are known.

Both the predictor and corrector are of the form,

$$c_i n_{i-1} + b_i n_i + a_i n_{i+1} = d_i \tag{1}$$

There are N of these equations in the system, where N is the number of solution points on the field line. A recursion relation is defined as,

$$n_i = E_i n_{i+1} + F_i \tag{2}$$

where E_i and F_i are quantities to be determined. If the above recursion relation holds, then $n_{i-1} = E_{i-1} n_i + F_{i-1}$. Substitution into (1) gives,

$$c_i E_{i-1} n_i + c_i F_{i-1} + b_i n_i + a_i n_{i+1} = d_i$$

Solving for n_i the following is obtained,

$$n_i = [-a_i / (b_i + c_i E_{i-1})] n_{i+1} + (d_i - c_i F_{i-1}) / (b_i + c_i E_{i-1})$$

Then by comparison with the defined recursion relation,

$$E_i = \frac{-a_i}{b_i + c_i E_{i-1}} \quad F_i = \frac{d_i - c_i F_{i-1}}{b_i + c_i E_{i-1}} \tag{3}$$

Before discussing the solution of the tridiagonal system, the method of handling the boundary conditions must be mentioned.

At the lower boundary, chemical equilibrium is imposed by setting production equal to loss,

$$p = \beta n \tag{4}$$

Therefore, the ionization density is,

$$n = p/\beta = \left[\frac{(p + \sqrt{p(p + 4w_1 w_2)})}{2w_1} \right] \tag{5}$$

where

$$\left. \begin{aligned} w_1 &= k_1[N_2] + k_2[O_2] \\ w_2 &= -k_2[O_2]/a_1 + k_1[N_2]/a_2 \end{aligned} \right\} \quad (6)$$

The numerical scheme uses index number one at the lowest altitude, therefore n_1 is the lowest altitude density value and is given from equations (5) and (6), and E and F at the lower boundary are set to,

$$E_1 = 0 \quad F_1 = n_1 \quad (7)$$

At the upper boundary, a field aligned ion flux F is taken as the boundary condition. The expression for the vertical ambipolar diffusion velocity w results in,

$$F \sin(I) = -D \partial n / \partial t - nD \left((1/T_p) \partial T_p / \partial z + 1/H_p \right) + n w_D \quad (8)$$

The boundary condition is therefore,

$$\partial n / \partial t = \left(w_D - (1/T_p) \partial T_p / \partial z - 1/H_p \right) n - (F \sin(I)) / D$$

It is assumed that F is a constant during a given time step, which is typically about 60secs. The boundary condition now has a linear form,

$$\partial n / \partial z = \alpha n - \gamma \quad (9)$$

where $\alpha = w_D / D - (1/T_p) \partial T_p / \partial z - 1/H_p$ and $\gamma = (F \sin(I)) / D$ are constants.

If the first order approximation $\delta n / \delta z|_N = (n_N - n_{N-1}) / \Delta z$ is used, the resulting solutions are found to depend largely on Δz , ie the solutions are dependent on the vertical step size, an undesirable feature. Therefore, a second order approximation to $\delta n / \delta z|_N$ must be made. An artificial point above the upper boundary point N+1 is defined such that the boundary condition (9), the diffusion equation (1), and the recursion relation (2), are also satisfied at the Nth boundary point. Since the exact location of the upper boundary point is not critical, the shift of the N+1 \rightarrow N and N \rightarrow N-1 points has negligible effect. The boundary value n_N is actually set at n_{N-1} value.

Equation (9) is then used to obtain,

$$\frac{n_N - n_{N-2}}{2 \Delta z} = \alpha n_{N-1} - \gamma \quad (10)$$

where α and γ are evaluated at the (N-1)th point.

As mentioned above, the recursion formula and diffusion equations must be satisfied. They are,

$$\left. \begin{aligned} n_{N-1} &= E_{N-1} n_N + F_{N-1} \\ a_{N-1} n_N + b_{N-1} n_{N-1} + c_{N-1} n_{N-2} &= d_{N-1} \end{aligned} \right\} \quad (11)$$

Solving equations (10) and (11) simultaneously for n_N results in,

$$n_N = \frac{d_{N-1} - 2\Delta z \gamma c_{N-1} - F_{N-1}(b_{N-1} - 2\Delta z \alpha)}{2/(\Delta z)^2 + E_{N-1}(b_{N-1} - 2\Delta z \alpha c_{N-1})} \quad (12)$$

It is interesting to note that the requirement for second order accuracy on the Neumann boundary condition results in a Dirichlet boundary condition.

At this upper boundary it has been necessary to set the ion flux as a function of the ion density. The results of Geisler(1967) have been used, viz the flux F is proportional to $n^{5/8} T_i^{3/2}$. The constant of proportionality was chosen such that a flux F of $10^8 \text{ cm}^{-2} \text{ s}^{-1}$ occurs when $n=2 \times 10^4 \text{ cm}^{-3}$ and $T_i=1500^\circ \text{K}$, which are approximate experimentally observed conditions. A similar procedure was used by Watkins and Richards(1979) and Schunk et al (1976).

In summary, the following sequence is followed to solve the O^+ diffusion equation.

- (1) Compute the lower boundary density n_1 using equation (2), then set $E_1=0$ and $F_1=n_1$
- (2) Compute the coefficients f_1, f_2, f_3, f_4 in the diffusion equation.
- (3) Compute the tridiagonal matrix elements and right hand vector components using equation(1) and equation (0a) predictor step, or equation (0b) corrector step.
- (4) Scanning from $i=2$ to $i=N-1$, compute the E_i 's and F_i 's using equation (3).
- (5) Using equation(12) to compute the upper boundary density n_N .
- (6) Scanning from $i=N$ to $i=2$, compute the new n_i 's using equation(12).

The steps (2) to (6) are performed for both the predictor and corrector steps. The predictor-corrector scheme is executed once for each time step.

1.2.3 AURORAL IONIZATION

Ionization from precipitating auroral particles is not as important as photoionization in magnitude, but plays an important role in defining the ionization structure on the nightside of the earth when photoionization is absent or minimal.

On the dayside auroral oval, the average energies are several hundred eV, resulting in ionization that peaks at altitudes 250 to 300 km. The results of Banks et al (1974) for 450eV electrons with a total flux of $1.5 \times 10^8 \text{ cm}^{-2} \text{ s}^{-1}$ have been used. The use of these results is a somewhat empirical approach, however it is quite time consuming to compute ionization rates from such low energy particles. In essence, we have directly adopted the ionization production rate from Banks et al for the low energy dayside auroral input. The ionization rate per unit flux for 450eV electrons has been scaled up for the flux mentioned above. The flux was chosen to give a peak density value about 10^5 cm^{-3} . Usually, the dayside auroral oval is at least partially sunlit, and auroral effects are very small compared to the background. The only exception is near mid-winter at longitudes near 100 degrees east where there is maximum separation the geographic and magnetic poles.

On the night side auroral oval, the characteristic energies are much higher, typically about 4 to 5keV. Code has been written that will determine the ionization profile from any arbitrary energy spectrum for energies down to a minimum of 500eV. For this initial work, a Maxwellian energy distribution with 5keV characteristic energy was used.

The following text summarizes the derivation of the production rate due to energetic electron precipitation, and the soft electron production rates that have been used.

(a) ENERGETIC ELECTRONS (> 500 eV)

(i) Definitions

- E electron energy
- $\epsilon(E)$ electron energy distribution function
- F_0 total electron flux
- z altitude
- $\rho(z)$ mass density
- $s(z)$ scattering depth = $\int^\infty \rho(z') dz'$
- $R(E)$ range function, see Barrett and Hays(1976) for values
- $\Lambda(s(z)/R(E))$ energy dissipation function
- $\epsilon(z)$ energy deposition rate per unit volume
- $q(z)$ total ionization rate of all species due to energetic electrons
- $q_0(z)$ ionization rate of O due to energetic electrons, the subscript denotes the species

(ii) Derivation

The differential rate of energy deposition per unit volume by the electron population $z(E)$ is,

$$d\epsilon = E \Lambda[s(z)/R(E)] \rho(z)/R(E) dF$$

The differential flux is $dF = F_0 \epsilon(E) dE$, therefore

$$d\epsilon = F_0 E \epsilon(E) \Lambda[s(z)/R(E)] \rho(z) / R(E) dE$$

The total rate of energy deposition per unit volume at altitude z is therefore,

$$\epsilon(z) = F_0 \rho(z) \int_{E_{\min}}^{\infty} E \epsilon(E) \Lambda[s(z)/R(E)] / R(E) dE$$

where E_{\min} is the minimum contributing energy.

Adopting $\Delta E_{ion} = 35\text{eV}$ to be the average energy required to create an ion-electron pair, the total ionization rate (for all species N_2 , O_2 , O) is,

$$q(z) = \frac{F_e \rho(z)}{\Delta E_{ion}} \int_{E_{min}}^{\infty} E \epsilon(E) \Lambda[s(z)/R(E)] / R(E) dE$$

To compute the ionization rate of O alone, the following relation has been used,

$$q_{\text{O}}(z) = q(z) \left[\frac{0.56 n_{\text{O}}(z)}{0.92 n_{\text{N}_2} + n_{\text{O}_2}(z) + 0.56 n_{\text{O}}(z)} \right]$$

This expression takes account of the relative magnitudes of the ionization impact cross sections. Similar expressions apply to $q_{\text{N}_2}(z)$ and $q_{\text{O}_2}(z)$.

A Maxwellian energy distribution is assumed,

$$\epsilon(E) = \frac{E}{E_0^2} e^{-E/E_0}$$

where E_0 is the characteristic energy; a value of 5keV has been considered typical of nighttime aurora. A flux $F_e = 5 \times 10^9 \text{ cm}^{-2} \text{ s}^{-1}$ gives an ionization rate that produces a peak density value about $5 \times 10^5 \text{ cm}^{-3}$. Only the ionization of O species is computed.

(b) SOFT ELECTRON PRECIPITATION

Due to the discrete nature of the collision processes at energies below about 500eV , the semi-empirical method of Rees(1963) that was used for the energetic electrons is not applicable. That method assumed continuous energy losses. For low energies it is necessary to solve the electron continuity equation. Since this is a computationally intensive, the ionization profile of Banks et al (1974) for 'soft' aurora has been used.

Examples of the auroral production for the energetic and low energy cases are shown in figures 1 and 2 respectively.

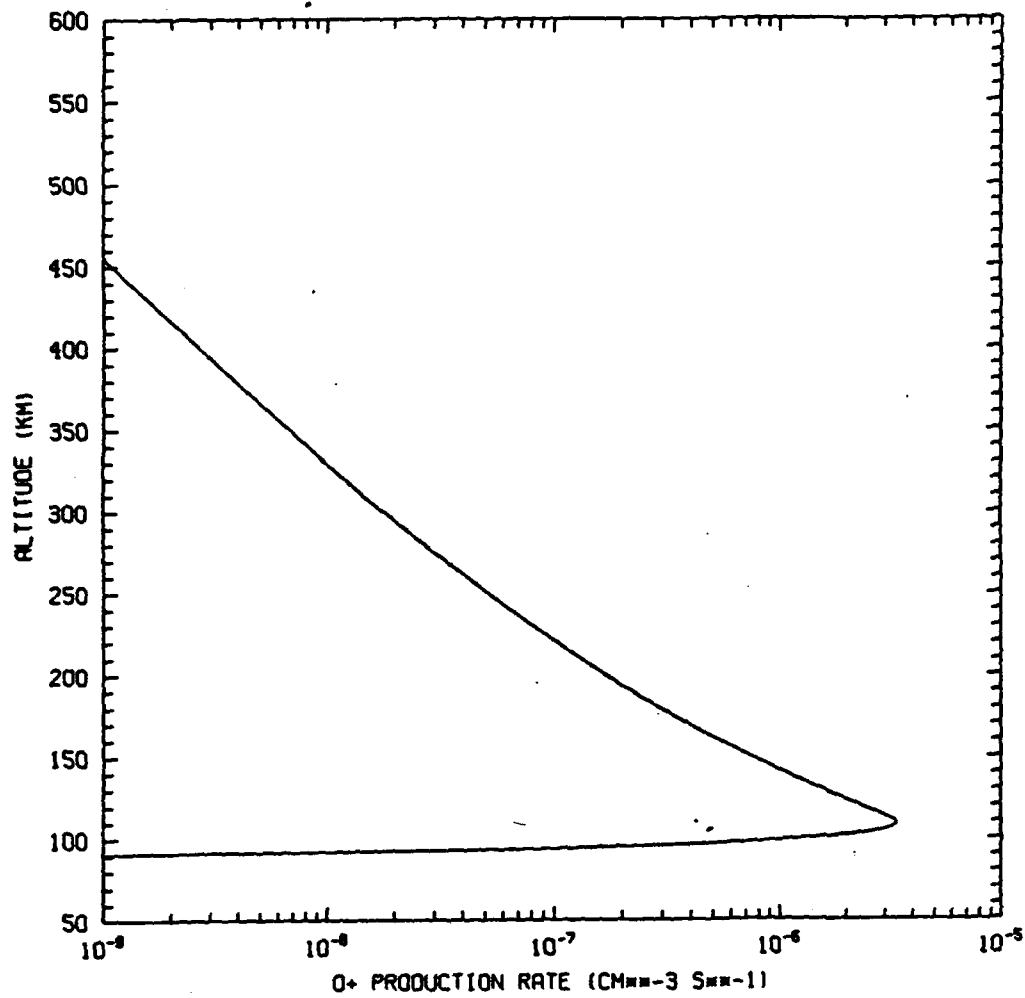


Figure 1 : Production rate of O^+ ions for a typical nighttime aurora. This is the production rate for unit flux. A Maxwellian energy spectrum with a 5keV characteristic energy has been assumed.

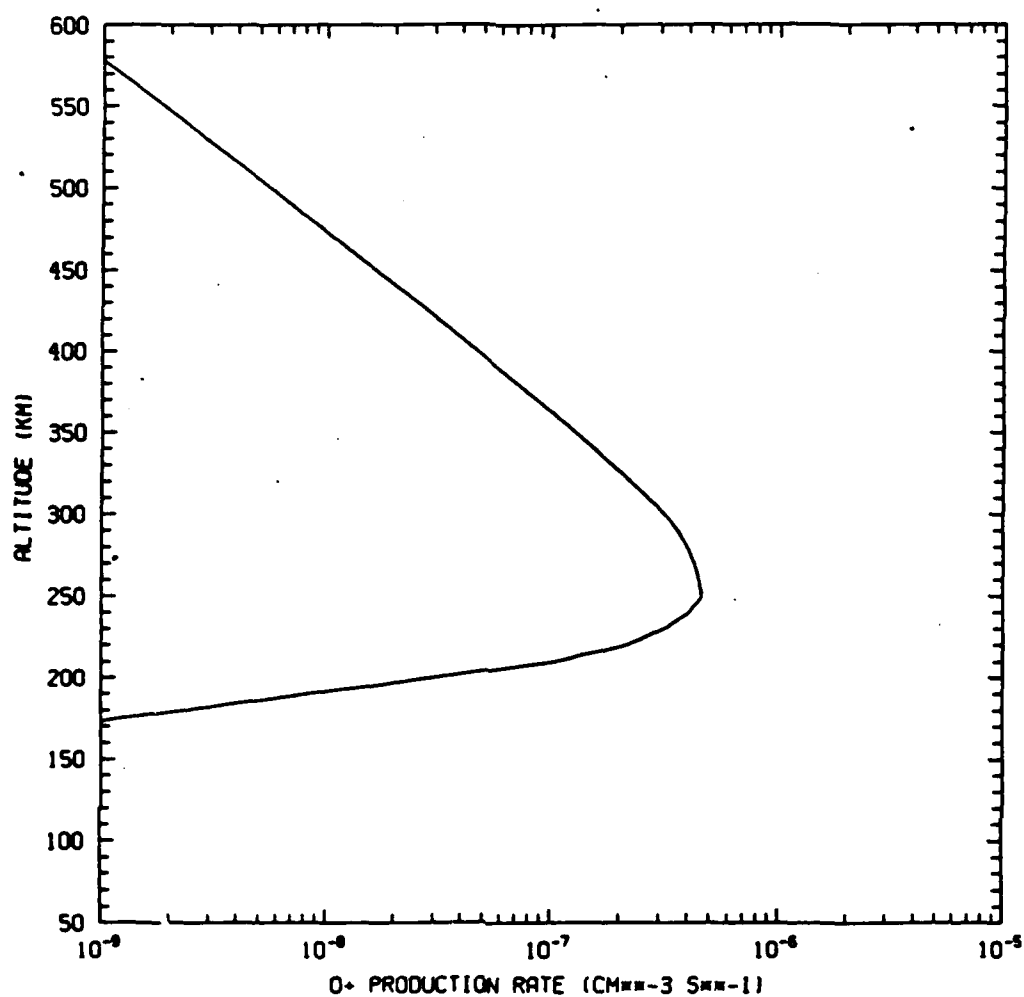


Figure-2 : Production rate of O^+ ions for a typical daytime aurora. This is the production rate for unit flux, and is the production that results from an 0.42keV monoenergetic energy spectrum.

1.3 CURRENT STATUS OF MODEL

The current version of the model incorporates the following processes.

- A magnetospheric model that determines the open field line region, and auroral oval precipitation region with the interplanetary magnetic field as input.
- A simple two cell convection pattern is used to define the large scale electric fields. The input may be defined with the magnitude of the cross polar cap potential, or the ϵ parameter (energy input from solar wind to the magnetosphere). The size of the electric field pattern is scaled to the size of the polar cap.
- The momentum and continuity equations for the major ion O^+ is solved vertically along inclined magnetic field lines. The MAGSAT magnetic field model that is based on spacecraft data has been used. The horizontal neutral wind is assumed equal to the horizontal $E \times B$ ion motion. The MSIS-86 neutral model that is derived from incoherent scatter radar and spacecraft data has been used for determining the neutral composition.
- The Air Force Geophysics Lab code is used to transform from the magnetic local time and magnetic latitude system, to the geographic system. In the geographic system, efficient code has been written to determine the solar zenith angle for any location at any time, and the photoionization rate as a function of altitude.
- Auroral precipitation may be determined on the nightside of the auroral oval from any input energy spectrum with energies down to 500eV. On the dayside auroral oval where energies are lower than 500eV the ionization rate is assumed to be from a mono-energetic 450eV flux of particles. The flux may be arbitrarily varied.
- Command files have been written for the VAX computer to run long simulations that compute the time varying ionosphere in response to time varying interplanetary field values.

1.4 MODEL APPLICATION

To illustrate the use of the model for time dependent applications, the ionospheric response to a large geomagnetic storm has been modeled over a 16 hour period and hourly results plotted.

1.4.1 IONOSPHERIC RESPONSE TO A GEOMAGNETIC STORM

Akasofu and Fry(1986) have developed a numerical solar wind code and applied it to examine the propagation of a major solar flare disturbance to the earth. The solar wind parameters at the earth several days after the flare are plotted in figure 3; the IMF and solar wind speed and density are shown. Using these solar wind parameters, the rate of energy input to the magnetosphere from the solar wind may be estimated from the ϵ parameter that was discussed in section 1.2. The total cross polar cap potential Φ is related statistically to ϵ by the relation that was also presented in section 1.2. The IMF coordinate system is shown in figure 4 because polar coordinates are used in the computations and plotted in figure 3; their relation to the more popular cartesian usage (B_x, B_y, B_z) is shown.

The results of the ionospheric response to the disturbance was computed and plotted each hour. This storm simulation was done for a day in January, and for a year in mid solar cycle. As the IMF changes the polar cap position and area changes; for the times 0200 to 1600 UT the positions are shown in figure 5. Each plot has magnetic latitude circles at 50,60,70,80 degrees, midnight (00MLT) is at the bottom, with 1200MLT at the top of each plot. The area of the polar cap expands to a maximum at about 0700UT when the B_z component of the IMF is most southward. The polar cap movements left and right on the figures results from the varying B_y component of the IMF.

The ion equations are solved in one minute time steps, and each individual field line is stepped in 3 minute increments along plasma convection paths. The entire three dimensional ionization structure is stored at hourly intervals and the data at 300km altitude is contoured and plotted. These hourly plots, which are shown in figures 6a to 6o, span the same time period as the figure 5. Initially in figure 6a, dayside ionization extends partially over the central polar cap, and on the nightside south of the auroral oval there is an ion density depletion (trough) with densities as low as $6 \times 10^3 \text{ cm}^{-3}$ at 1900MLT and 62 degrees magnetic latitude. During most of the nighttime period the trough is located at 55-60 degrees latitude with density values about $8 \times 10^3 \text{ cm}^{-3}$. The peaks in ionization density from 0200 to 0500MLT at 70 degrees latitude, and 1900 to 2100MLT at 75 degrees latitude are caused by auroral precipitation. Although most auroral ionization occurs at about 110km altitude, there is sufficient production up to 250km that diffuses upward to enhance the F region densities at 300km and higher; this can occur because the convection velocities are parallel to the auroral oval at those locations and there is sufficient time for ions to diffuse upward. The decrease in this auroral 'hill' occurs near midnight because the convection there tends to be perpendicular to the auroral oval and there is less time for vertical diffusion of auroral ionization to take place.

In the following time sequence of plots there is a great deal of structure. As the cross polar cap potential increases it tends to rapidly transport plasma from the dayside across to the nightside auroral zone. This becomes quite extreme in figure 6f for example where the densities at 60 degrees latitude have increased by a factor of about ten, and the nightside trough formerly at 50 to 65 degrees latitude has disappeared. The densities equatorward of 52 degrees drop rapidly into the region where corotating magnetic field lines that have been relatively unaffected by the disturbance and recombination has had sufficient time to act so that densities as low as $1 \times 10^4 \text{ cm}^{-3}$ are present.

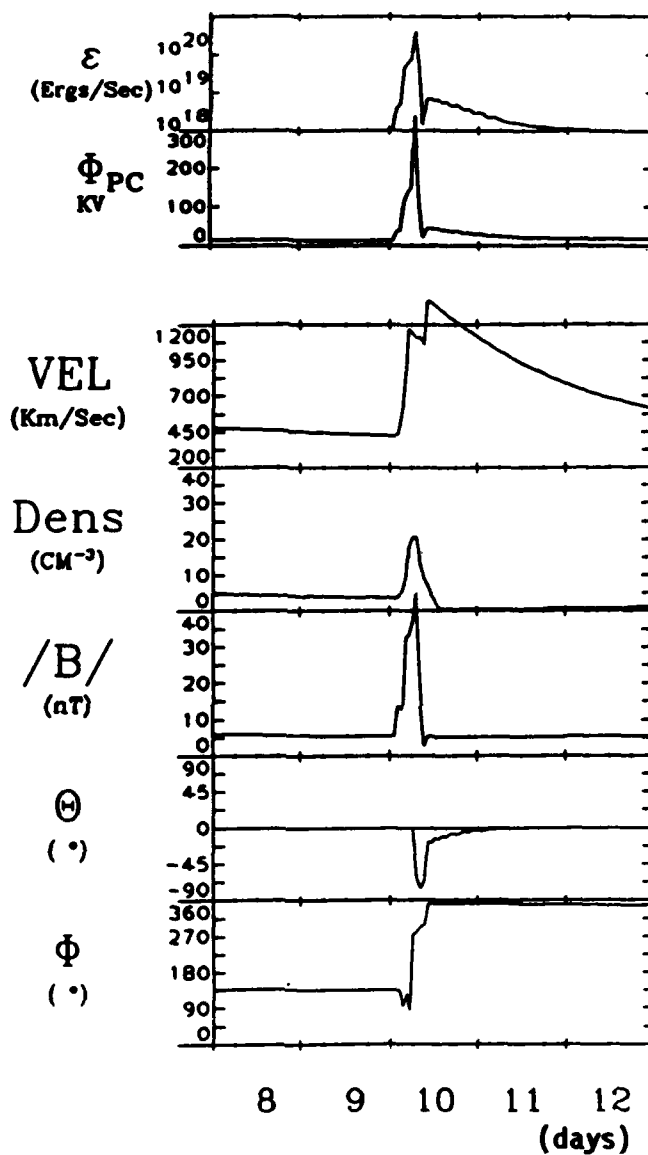


Figure 3. Model geomagnetic storm parameters from Akasofu and Fry(1986) that have been used for inputs to the ionospheric model. The lower 5 parameters are solar wind velocity, density, and magnetic field. The top two parameters are computed from the solar wind data. These values are plotted for 5 days after a solar flare.

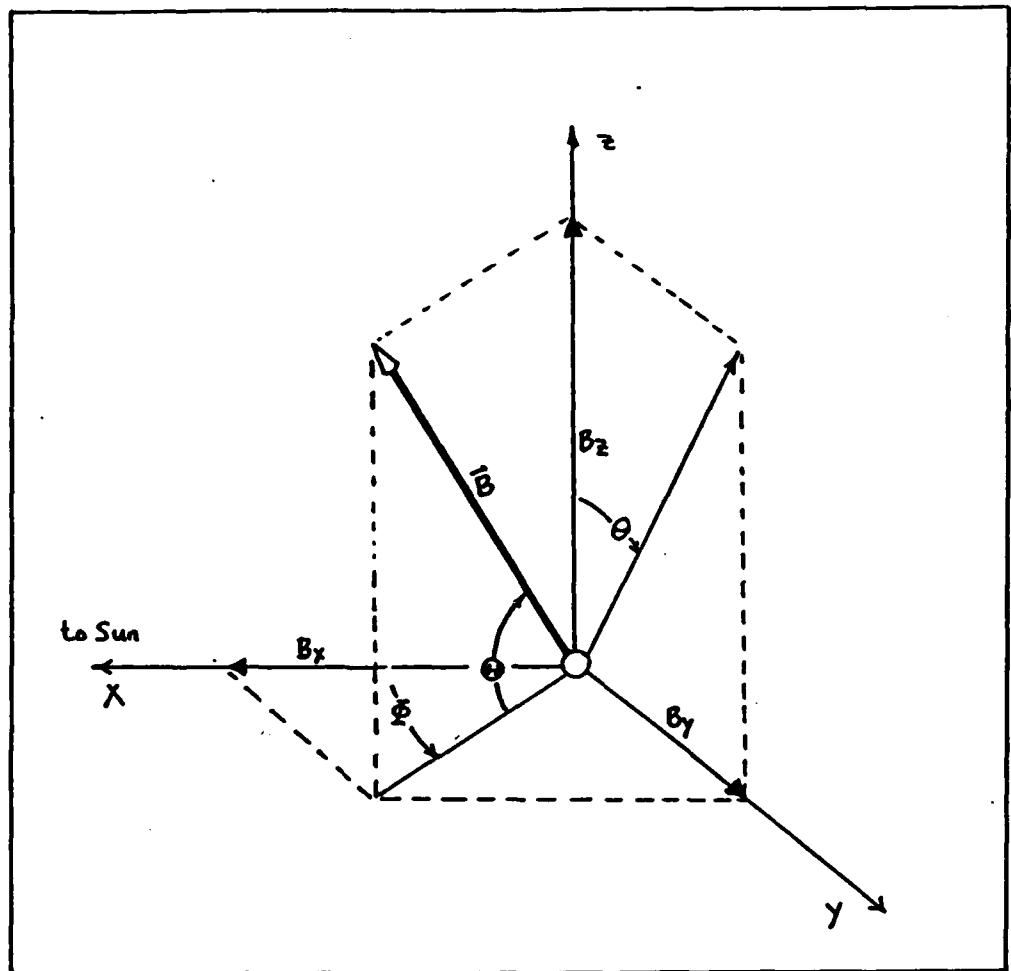


Figure 4. The magnetic coordinate system used for the solar wind data in figure3. The earth is the small sphere.

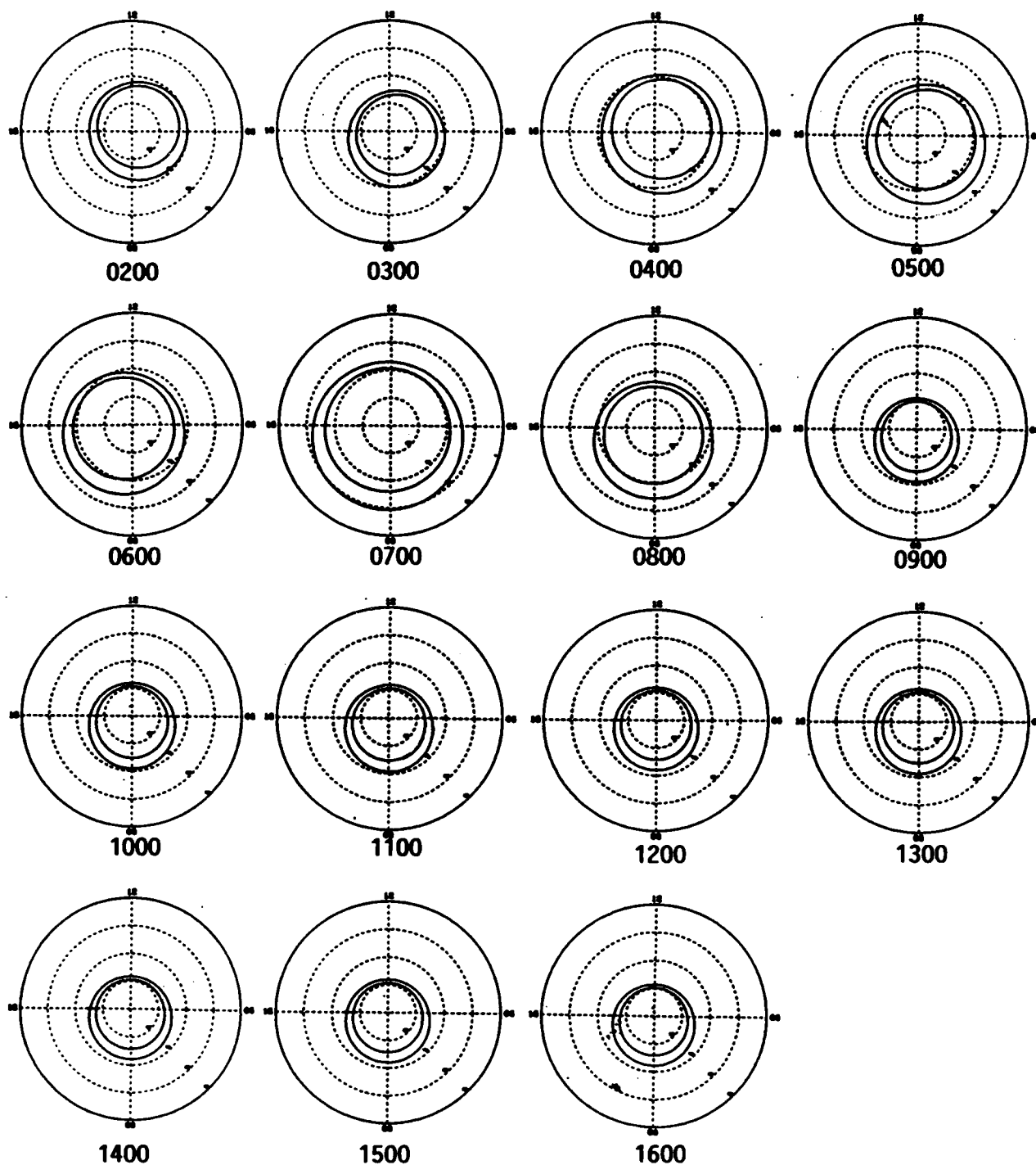


Figure 5. Time dependent behavior of the polar cap in response to the varying interplanetary magnetic field in figure 3. The times are UT on day 10 shown in figure 3.

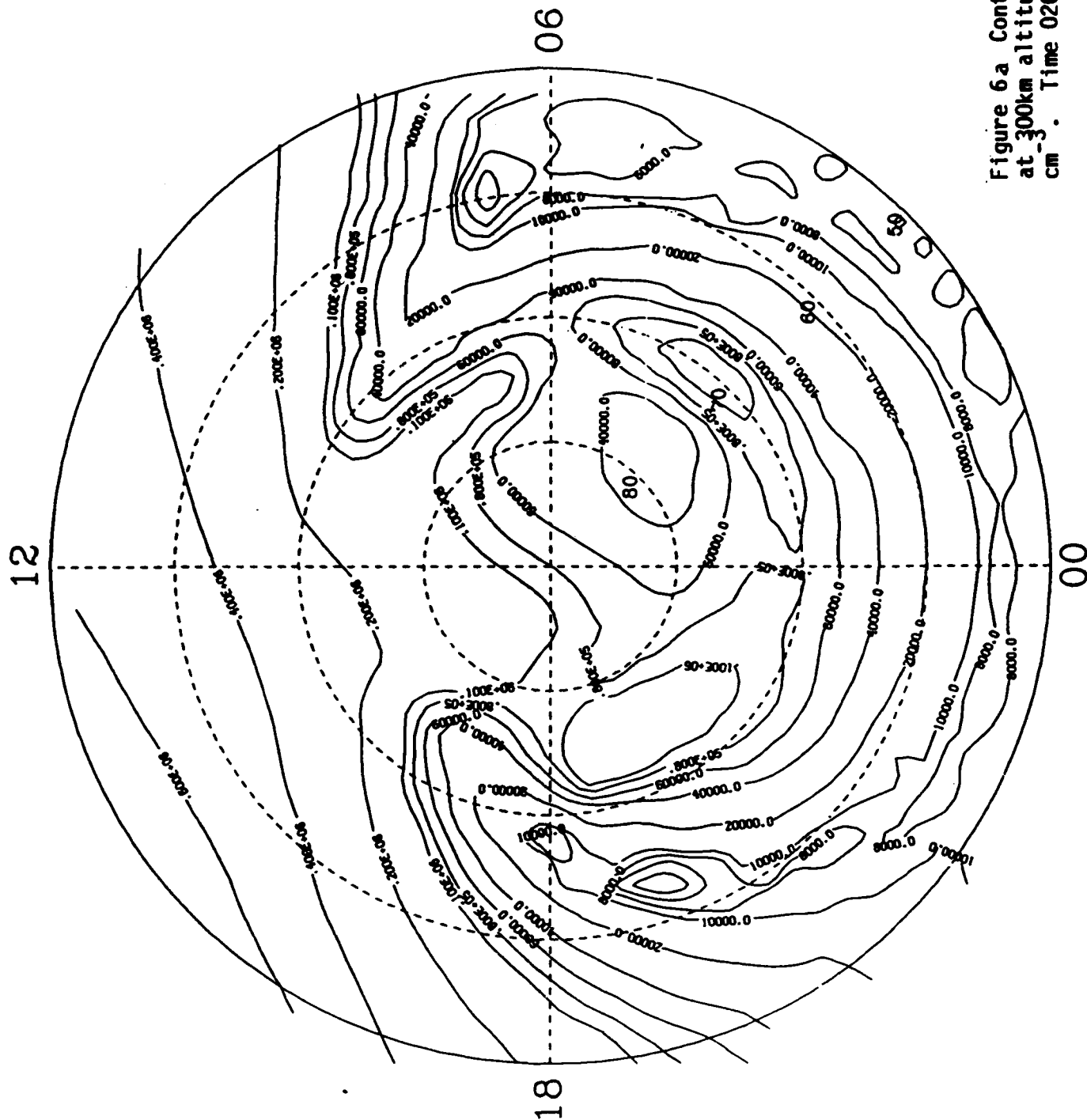


Figure 6a Contours of ion densities
at 300km altitude in units of
cm⁻³. Time 0200UT.

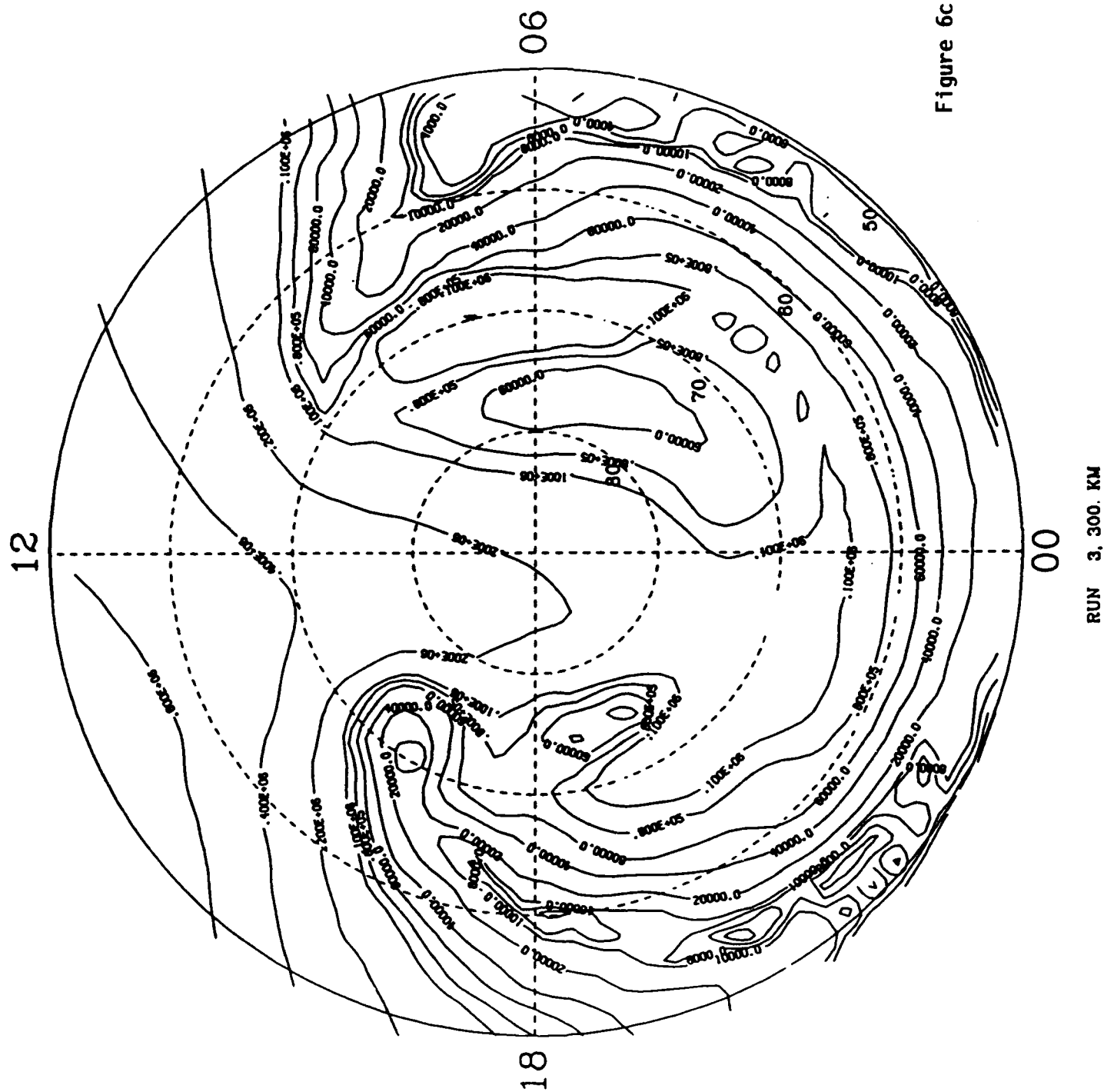


Figure 6c. 0400UT



Figure 6d. 0500UT

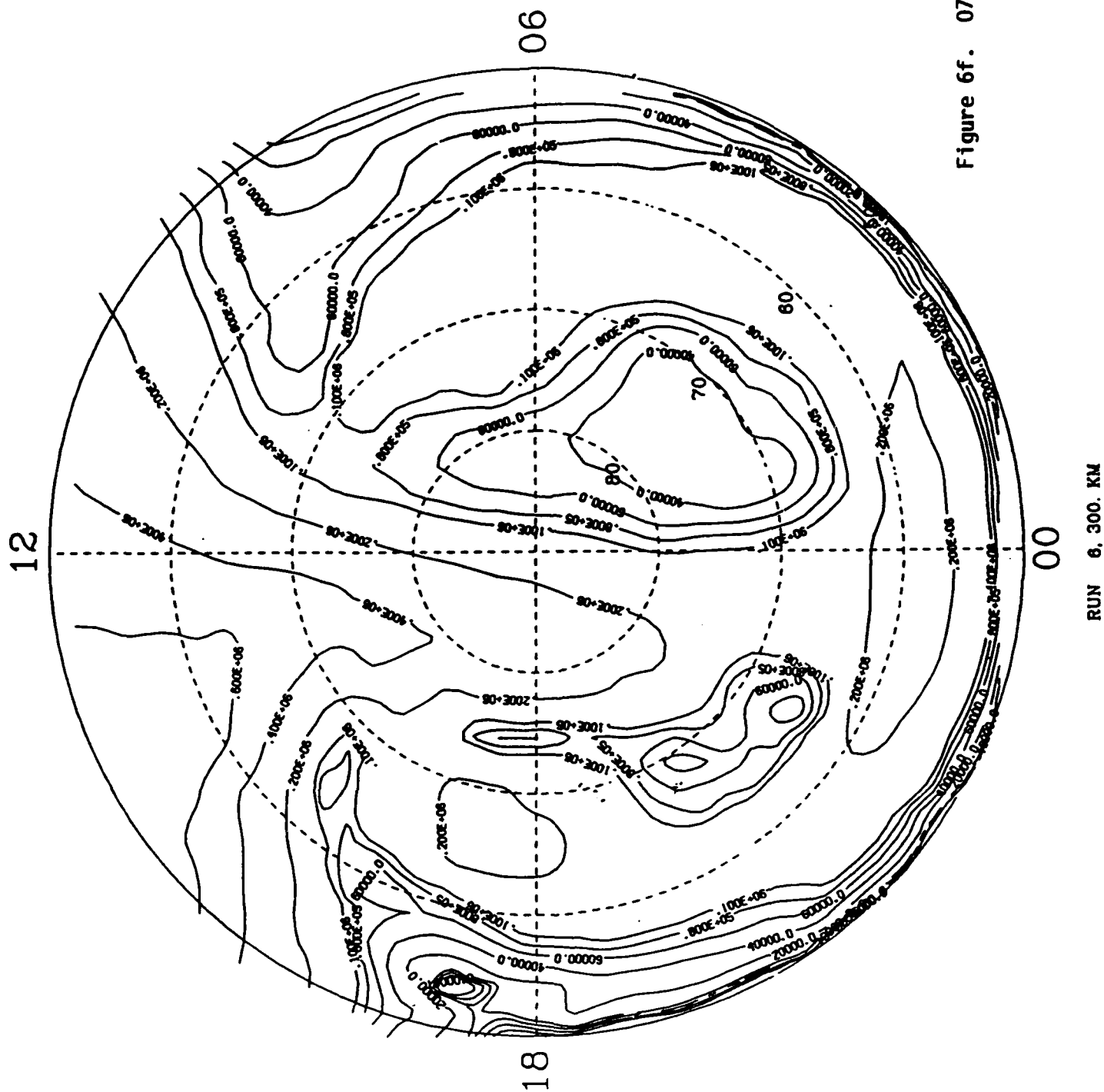


Figure 6f. 0700UT

RUN 6, 300. KM

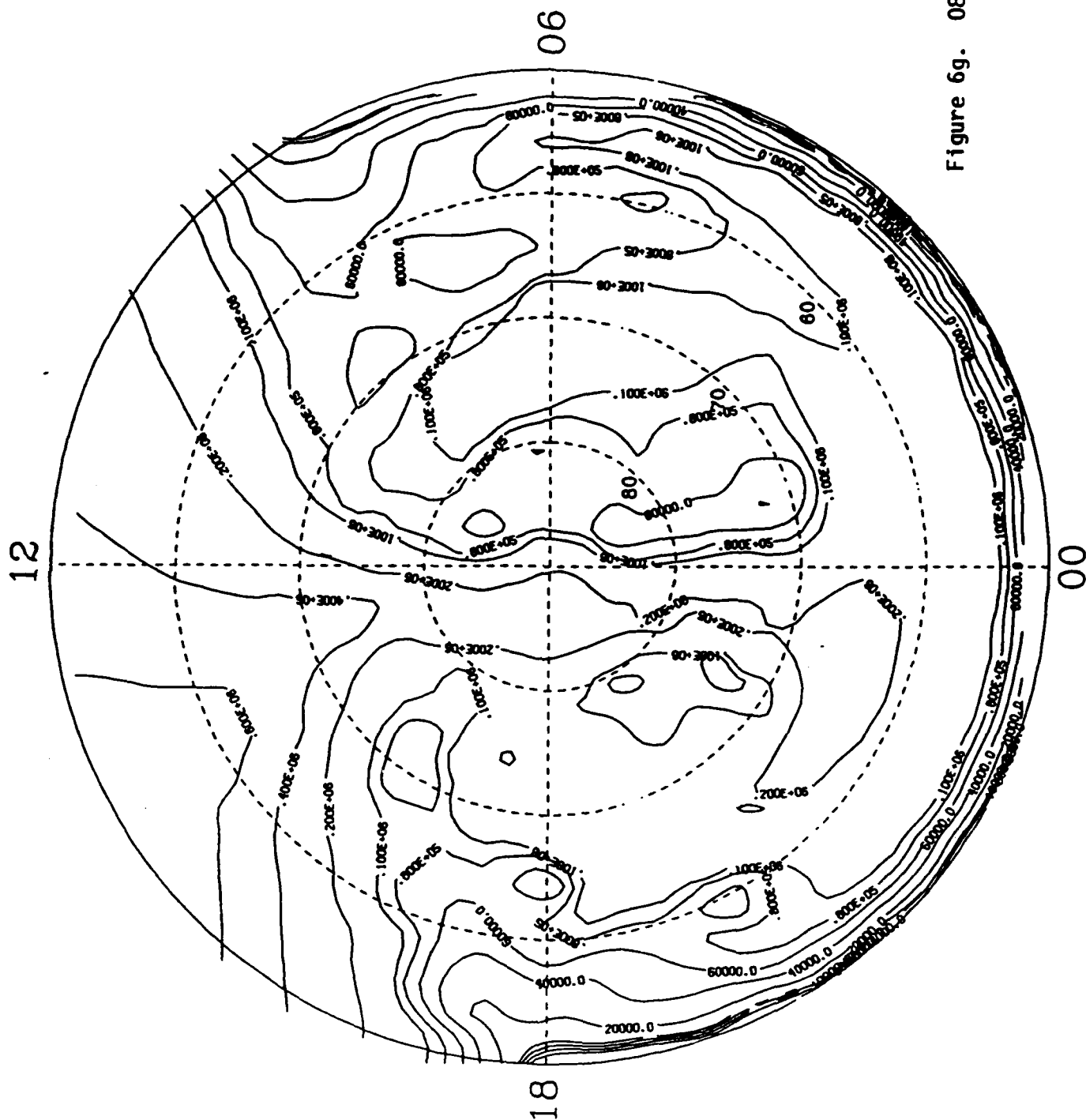


Figure 6g. 0800UT

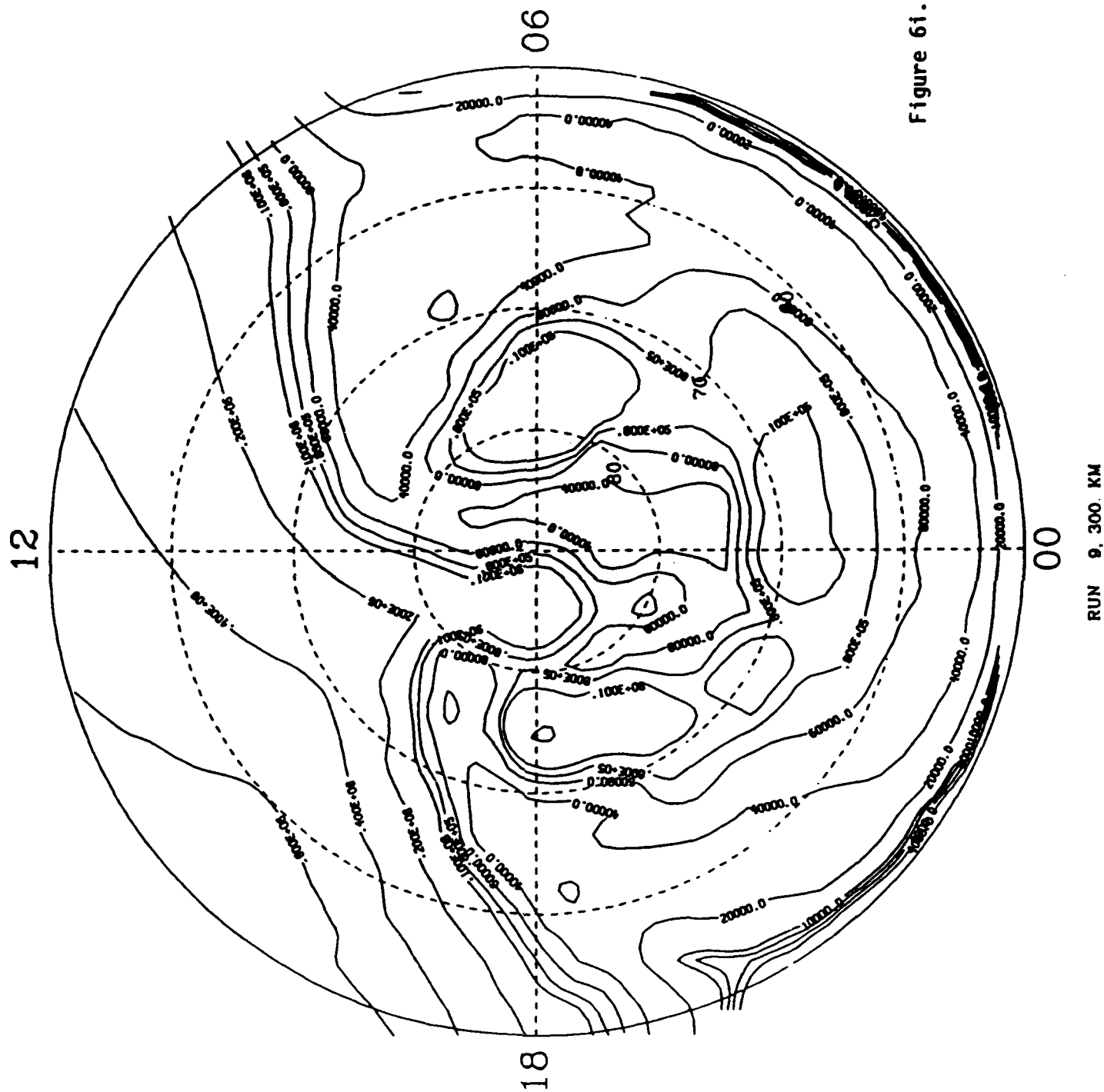


Figure 6i. 1000UT

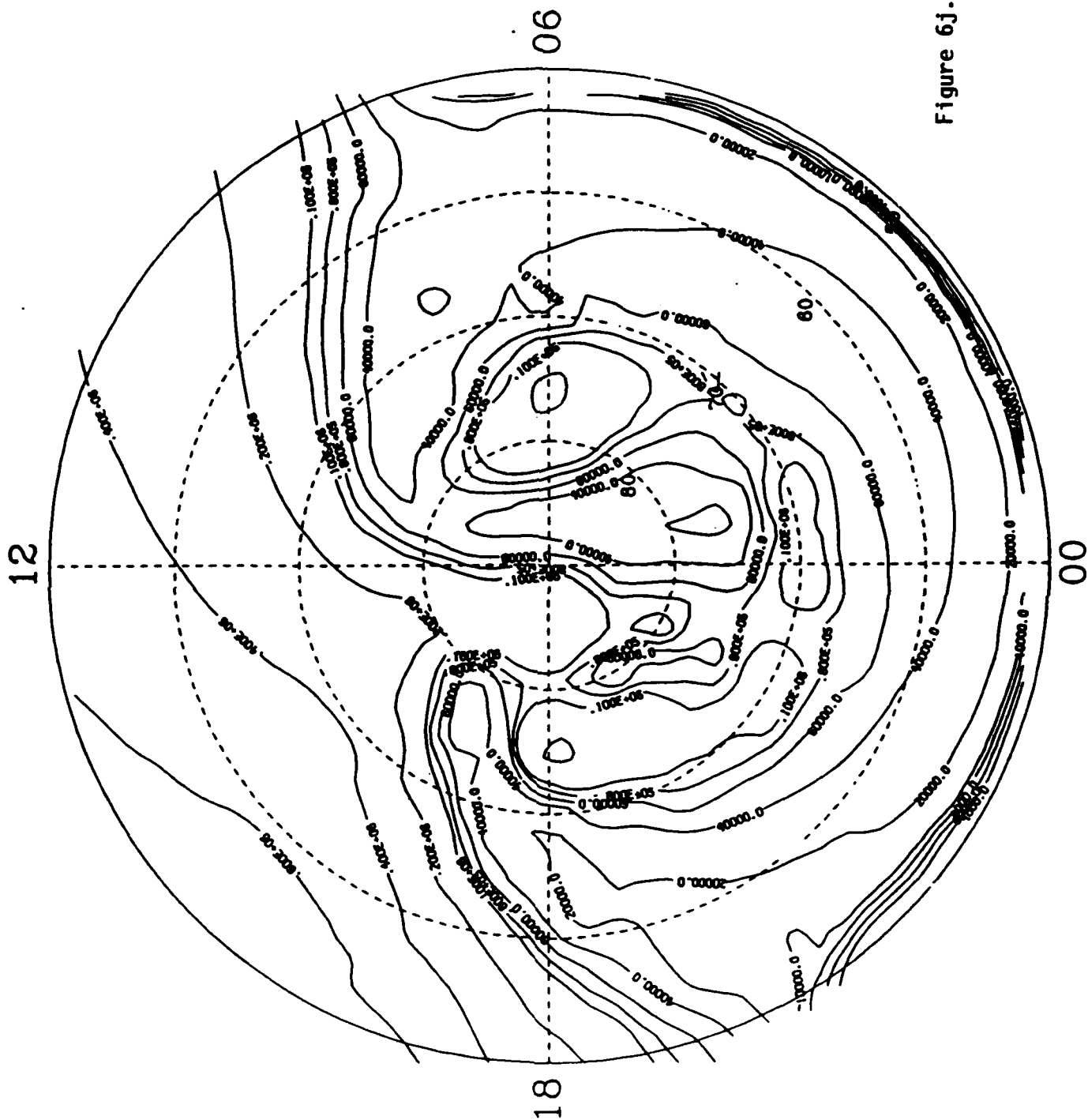
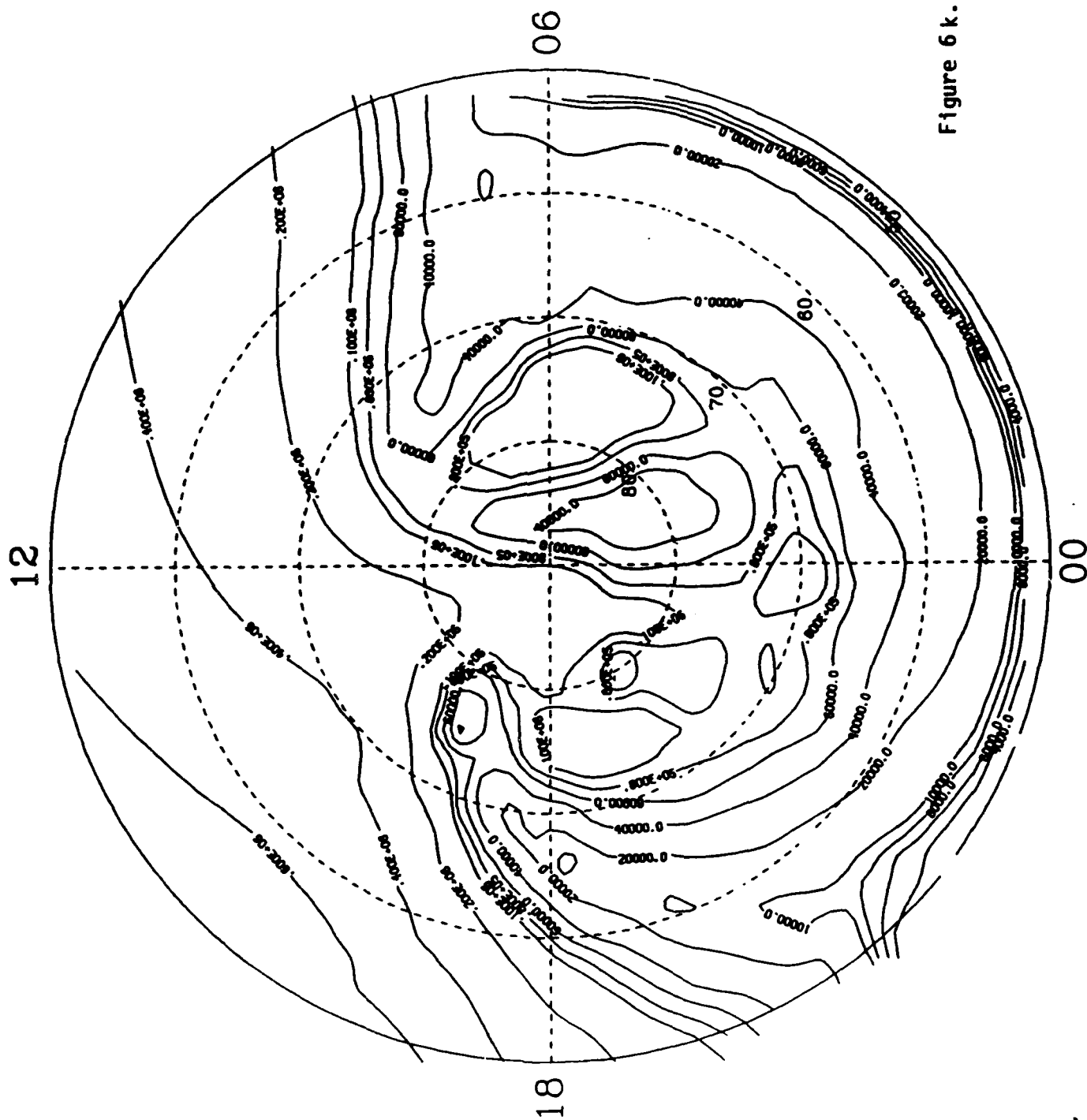


Figure 6j. 1100UT



RUN 11, 300. KM



Figure 6n. 1500UT

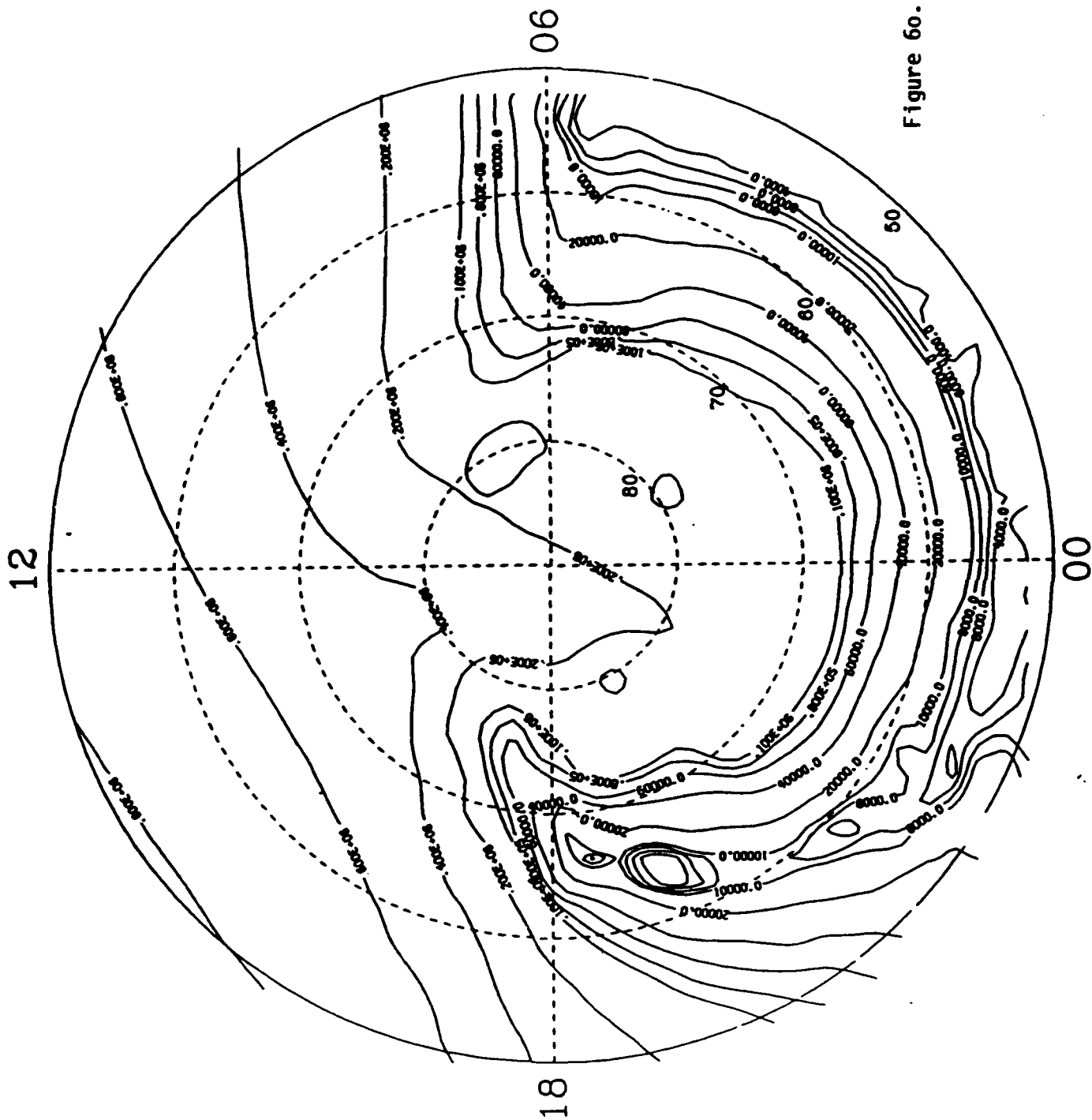


Figure 60. 1600UT

RUN 15, 300. KM

2. PLANNED MODEL EXTENSIONS AND APPLICATIONS

During the latter portion of the grant period some planning had been made for extending the model. There are three limitations that must be addressed before the model can be used for realistic comparisons with data or for predictive purposes.

(i) Electric Fields

The simple two cell convection pattern that has been used is a reasonable representation of the actual average situation. However, a model based on real data has been kindly given to us by Dr Heelis at University of Texas. It is based on data from the Dynamics Explorer spacecraft and represents the statistical results of comparisons with the interplanetary field. It was only acquired in July 1987 and therefore there was insufficient time to incorporate it into the current version of the model.

(ii) Multiple Ion Species

The current effort only solves for O^+ ions. There are two other minor ions in the F region, O_2^+ and NO^+ that should be incorporated. The NO^+ ions are particularly important during magnetically disturbed periods because their production is enhanced to the level where their concentration may significantly affect the recombination rate.

(iii) Neutral Winds

The dynamics on the neutral gas should be self consistently computed with the ion motions. The particular situation that occurs when the neutral wind is north-south with a magnitude that is different to the ion drift motion will affect ionospheric densities. When a neutral wind is blowing from north to south, ion drag forces tend to move ions up or down the inclined magnetic field lines. For an upward drift, ions are moved to higher altitudes where the recombination time is longer and this results in higher ion densities and a higher altitude peak in the density height profile. For a downward drift the reverse occurs, ie movement of ions to lower altitudes resulting in greater recombination and lower ion densities.

With regard to applications of the model, it is planned to concentrate on comparisons with real data, probably incoherent-scatter radar density and electric fields, and spacecraft particle data to determine the auroral particle input fluxes. The polar cap region is particularly interesting because of the complex ionization structures that have been observed. With greater spatial resolution understanding of the formation and evolution of polar cap structures should be possible.

3. PERSONNEL

The initial work on this grant was performed by the principal investigators; Professor Akasofu developed the magnetospheric model and Dr Watkins was responsible for the convection electric field model, coupling the magnetospheric model to the convection model, developing code to step along equipotentials, and the initial code to solve the ion equations. In July 1986 we recruited a new PhD student, Mr Chris Grimm. He has spent a large amount of time learning to use the existing code, has greatly enhanced the efficiency of the ion equation code, and has written code for computing the auroral ionization. Mr Grimm is a very competent programmer and has also been of assistance in packaging the various programs to run from a command file on the Geophysical Institute's VAX computer. He has also taken the Aeronomy course at the Geophysical Institute and has begun to contribute scientifically to our effort. It is anticipated that this research will continue and subsequent results will form the basis for Mr Grimm's thesis. The grant has been very valuable in introducing a new researcher to the field.

4. EXTERNAL INTERACTIONS

4.1 CONFERENCE PRESENTATIONS

Four conferences have been attended and papers presented.

(a) NATO Advisory Group for Aerospace Research, 36th Symposium, Fairbanks, Alaska, June 1985.

Paper titled 'Progress in Modeling the Polar Ionosphere from Solar and Magnetospheric Parameters'

(b) Ionospheric Effects Symposium on 'The Effects of the Ionosphere on Communication, Navigation, and Surveillance Systems', May 1987.

Paper titled 'A Numerical Prediction of Ionospheric Conditions After an Intense Solar Flare'

(c) XXII General Assembly of the International Union of Radio Science.

Paper titled 'Dynamic Ionospheric Models'

4.2 PUBLICATIONS

The following are in various stages of the publication process.

(a) 'Progress in Modeling the Polar Ionosphere from Solar and Magnetospheric Parameters', NATO Advisory Group for Aerospace Research, Report No 382, 1986, by Watkins, Akasofu and Fry.

(b) 'A Numerical Prediction of Ionospheric Conditions After an Intense Solar Flare', in press, in proceedings of symposium on The Effect of the Ionosphere on Communication, Navigation, and Surveillance Systems, 1987, by Watkins and Akasofu.

(c) 'Numerical Modeling of Magnetic Storm Effects on the Polar F-Region Ionosphere', in preparation for special issue of Radio Science, by Watkins, Akasofu and Grimm.

4.3 PARTICIPATION IN THE 'CEDAR' PROGRAM

The CEDAR (Coupling, Energetics, and Dynamics of Atmospheric Regions) science effort is an NSF initiated program with three major goals. These are, first to study the dynamics and energetics of the upper atmosphere from the mesopause upward to the exobase (about 80 to 150km altitude), second to study mesospheric-thermospheric coupling, and third to study ionosphere-magnetosphere-thermosphere coupling.

Within the CEDAR program there are a number of individual smaller efforts that will contribute to the overall objectives. One of these, organized by Dr S. Basu at Air Force Geophysics Lab, called HLPS (High Latitude Plasma Structures), is directed toward understanding the physical processes responsible for the formation and evolution of polar cap ionization structures. This modeling effort will be an important contribution.

5.0 CONCLUSIONS

This grant has been very successful and is the first attempt to couple a magnetospheric model to a large-scale ionospheric model. The codes are quite efficient and may be run efficiently on a VAX computer of the 780 size or larger when the horizontal grid spacing is at least 5 degrees of latitude and 5 degrees of longitude; the vertical grid size is now 10km which should remain fixed. If better spatial resolution could be realized by using greater computing resources, it should be possible to study small-scale polar cap structures, both their formation and evolution. Time dependent simulations of a large magnetic storm show very complex time dependent behavior of the ionosphere.

In future, further extensions of the model to include neutral wind effects and multiple ions should permit many useful insights into the physical processes operating in the polar ionosphere. Comparisons with real data, and the application of the model for predictive purposes should then be possible.

REFERENCES

- Akasofu, S.-I., and M.Roederer, Dependence of the polar cap geometry on the IMF, Planet. Space Sci., 32,p111,1984
- Barrett, J.C., and P.R.Hays, J. Chem Phys., 64, 2, 1976.
- Banks, P.M., C.R.Chappell, and A.F.Nagy, J. Geophys. Res., 79, p1459, 1974.
- Geisler, J.E., J. Geophys. Res., 72, p81, 1967.
- Rees, M.H., Planet. Space Sci., 11, p1209, 1963.
- Reif, R.J., R.W.Spiro, and T.W.Hill, Dependence of Polar Cap Potential Drop on Interplanetary Parameters, J. Geophys. Res., 86, p7639, 1981.
- Schunk,R. W., P.M. Banks, and W.J.Raitt, J. Geophys. Res., 81, p3271, 1976.
- Watkins, B. J., and P. G. Richards, J. Atmos. Terres. Phys., 41, p179, 1979.

END

11-87

DTIC